Atmos. Chem. Phys. Discuss., 9, 5465–5503, 2009
www.atmos-chem-phys-discuss.net/9/5465/2009/


Atmospheric Chemistry and Physics Discussions

This discussion paper is/has been under review for the journal *Atmospheric Chemistry and Physics (ACP)*. Please refer to the corresponding final paper in *ACP* if available.

# How important is the vertical structure for the representation of aerosol impacts on the diurnal cycle of marine stratocumulus?

**I. Sandu[1,2], J.-L. Brenguier[1], O. Thouron[1], and B. Stevens[2,3]**

[1]CNRM-GAME, Meteo-France/CNRS, Toulouse, France
[2]Max Planck Institute for Meteorology, Hamburg, Germany
[3]University of California at Los Angeles, Los Angeles, CA, USA

Received: 19 December 2008 – Accepted: 8 February 2009 – Published: 2 March 2009

Correspondence to: I. Sandu (irina.sandu@zmaw.de)

Published by Copernicus Publications on behalf of the European Geosciences Union.

## Abstract

Large Eddy Simulations (LES) are performed to examine the impact of hygroscopic aerosols on the diurnal cycle of marine stratocumulus clouds, under varying meteorological forcing conditions. When the cloud condensation nuclei concentration increase is sufficient to inhibit drizzle formation in the cloud layer, the precipitating and the non-precipitating cloud layers exhibit contrasting evolutions, with noticeable differences in liquid water path. Aerosol induced modifications of the droplet sedimentation and drizzle precipitation result in noticeable changes of the entrainment velocity at cloud top, but also in significant changes of the vertical stratification in the boundary layer. This set of simulations is then used to evaluate whether a model which does not explicitly represent the effects of the interactions occurring within the boundary layer on its vertical stratification (i.e. such as a mixed layer model) is capable of reproducing at least the sign, if not the amplitude, of these aerosol impacts on the liquid water path. It is shown that the deviations from the mixed layer idealized state are crucial ingredients of the aerosol impacts so that a mixed layer model is unable to even replicate the sign of the liquid water path changes.

## 1 Introduction

The significant contribution of marine stratocumulus to the Earth's radiative budget has motivated in the last decades numerous observational and modeling studies of this important cloud type. Moreover, because these shallow boundary layer clouds are thought to be particularly sensitive to changes in the properties of the atmospheric aerosol, via the induced changes in their cloud droplet number concentration (CDNC) and their propensity to rain (i.e. aerosol indirect effects), special attention has been paid recently to their interactions with the aerosol loading. In this study, we are continuing this effort by focusing on the role played by an accurate representation of the stratocumulus-topped boundary layer's (STBL) vertical structure in the prediction of the aerosol effects on the cloud cover.

A characteristic feature of marine stratocumulus is that their vertical development is tightly confined by a low inversion layer so that the free troposphere above is barely affected by the clouds below (see Stevens, 2005, for a review). It is thus conceivable to consider the STBL as a separate system whose evolution is entirely governed by the energy fluxes at the surface and through the inversion layer. Indeed, this assumption of horizontal homogeneity underlies all STBL parameterizations with which we are familiar. By further assuming that the STBL is vertically uniform, or well mixed one arrives at an effectively 0-dimensional model first expounded by Lilly (1968). Lilly's mixed layer (ML) theory elegantly couples the cloud, radiative and turbulent processes. The main advantage of this framework is that, while the state of the free-troposphere is known, the cloud's bulk properties (i.e. liquid water path (LWP) and geometrical thickness) and the fluxes of moisture and heat at the boundaries can be easily derived from the bulk properties of the well-mixed layer, i.e. its depth and the values of the conservative variables: the liquid water potential temperature $\theta_l$ and the total water content $q_t$. This simple framework has already been used (Nicholls, 1984; Turton and Nicholls, 1987; Bretherton and Wyant, 1997; Stevens, 2000a, 2002; Lilly, 2002; Caldwell et al., 2005; Lilly and Stevens, 2008; Lilly, 2008) to provide a deep understanding of the STBL dynamics, and recently to explore aerosol indirect effects (Zhang et al., 2005; Wood, 2007). The mixed layer theory has also been criticized, principally because boundary layer clouds often exhibit important and significant departures from a well mixed state, particularly during the daytime (Nicholls, 1984), or in the presence of precipitation (Albrecht, 1993).

These criticisms resonate with recent results from large-eddy simulations (LES) which indicate that the evolution of marine stratocumulus, and more particularly their response to an increase of the aerosol loading, couples sensitively to the vertical structure of the STBL. For instance Sandu et al. (2008) showed that the differences between the diurnal cycles of a pristine precipitating and a polluted non-precipitating marine stratocumulus are tightly related to the differing evolution of the vertical structure of the respective STBLs. The evolution of the non-precipitating STBL corroborates the widespread image of the diurnal variation of such boundary layers, wherein the boundary layer is well-mixed during night and decouples during daytime. In the precipitating case, the sedimentation of condensed water affects this evolution, so that the STBL is poorly mixed during the night, when drizzle evaporates in the entire subcloud layer, and it is less decoupled than the non-precipitating one during the day, when drizzle evaporates completely just beneath the cloud base. Two mechanisms are responsible for this modification of the STBL's evolution in the precipitating case. Thus, as earlier argued by Stevens et al. (1998) and subsequently shown by a number of others (Ackerman et al., 2004; Lu and Seinfeld, 2005; Bretherton et al., 2007; Savic-Jovcic and Stevens, 2008), the sedimentation of drizzle and cloud drops reduces the cloud top entrainment. However, the evaporative cooling of drizzle drops under the cloud base modifies the stability of the STBL (see also Feingold et al. (1996)). The fluxes of heat and moisture at the boundaries of the STBL, which depend on the vertical structure of the boundary layer and on the entrainment rate, thus evolve differently in the pristine and, respectively, in the polluted case. As these fluxes control the evolution of the STBL, the two simulations diverge rapidly, although they start from the same state, and exhibit a less pronounced diurnal cycle in the pristine case.

This article builds off on this previous work and attempts to more quantitatively ask how important it is to account for the vertical structure of the STBL, which appears to be modulated by precipitation, in order to predict the contrasting evolutions of precipitating versus non-precipitating STBLs obtained with LES. In other words, we are questioning here whether a model which does not explicitly represent the effects of the interactions between drizzle evaporation, radiative transfer and dynamics on the STBL's vertical structure and coupling (i.e., the mixed layer theory of Lilly, 1968) is at least capable of reproducing the sign and reasonably well the amplitude of the LWP response to modifications of the precipitation process and the contrasting time evolutions of the two STBLs. While it may be clear that the assumption of well mixedness will distort the structure of the cloud layer for boundary layers that are not well mixed, it is by no means clear that such distortions will also be apparent in the differential response of the boundary layer to different aerosol concentrations.

Our methodology is the following. First, we perform three pairs of 72 h LES of pristine precipitating and polluted non-precipitating STBLs, which cover a broad range of meterological conditions (Sect. 2). The results of these simulations are then used to compute the bulk properties of the well-mixed layers that are equivalent to the bulk properties of the STBLs as represented by the LES. From these properties, we derive the bulk properties of the clouds that would develop in these well-mixed layers, and we compare them to the horizontally averaged properties of the clouds simulated at the same times. These comparisons will emphasize whether, while the bulk states of the well-mixed layers are correctly specified, the ML framework reproduces the differences between the pristine and the polluted clouds showed by the LES (Sect. 3). The next step consists in comparing the fluxes of heat and moisture at the boundaries of the equivalent well-mixed layers, computed within the ML framework, with the horizontal averages of the simulated fluxes. In order to quantify the impacts of the errors made by representing the different fluxes at the boundaries with the ML framework, we will discuss the errors that they would imply on the prediction of the difference in LWP between pristine and polluted clouds (Sect. 4). Finally, we use the ML theory to predict the evolutions of pristine/polluted STBLs and we compare the results with those obtained from LES (Sect. 5). Section six summarizes what we learned through the course of this exercise.

## 2 Large eddy simulations

To explore a broad range of meteorological conditions three pairs of LES of the diurnal cycle of the STBL are performed. External forcings typical of Northeast Pacific summertime stratocumulus regime are chosen. For each pair, a first simulation is ran for a duration of 75 h, starting at 21 local time (LT), with a cloud condensation nuclei (CCN) concentration typical of a pristine air mass, i.e. 50 $cm^{-3}$, that results in CDNC values of about 40 $cm^{-3}$. The same simulation is then replicated, but the CCN concentration is suddenly increased at midnight (i.e. after the spin-up period of 3 h) to a value of 600 $cm^{-3}$. The CCN activation scheme rapidly adjusts CDNC to this new CCN background, with CDNC values of about 200 $cm^{-3}$. These two classes of simulations are hereafter refereed to as PRIS and POL, respectively. The PRIS simulations always produce precipitation, while the CDNC increase in the POL set of simulations is sufficient to inhibit drizzle formation within a few hours after the CCN concentration has been changed. The first 12 h (from 00:00 to 12:00 LT on the first day of simulation) are disregarded in our subsequent analysis as we are not interested in the transient response to the sudden change in the CCN concentrations. The overall duration of each simulation, twice as long as in Sandu et al. (2008), was chosen in order to capture the effect of the time-varying boundary conditions and thereby provide a richer, hopefully somewhat more general, family of cases for study; particularly in light of past work that shows the planetary boundary layer (PBL) remembers its upstream environment for a day or more, e.g., Schubert et al. (1979); Klein and Norris (1995); Pincus et al. (1997). Note also that concomitant impacts due to aerosol absorbing properties (the semi-direct effect) are disregarded by choosing a single scattering albedo typical of cloud droplets formed on sulphate, which has a low absorption coefficient, similar to that of pure water.

### 2.1 The LES model

The numerical model used in this study is the three-dimensional LES configuration of the non-hydrostatic model Meso-NH (Lafore et al., 1998), described in detail in Sandu et al. (2008), which uses a grid mesh of 50 m on the horizontal and of 10 m on the vertical. This model solves a bulk microphysical representation of the cloud processes (using the parameterizations of Cohard et al. (2000a) for CCN activation, Khairoutdinov and Kogan (2000) for droplet autoconversion and accretion, and Geoffroy (2007) for droplet and drizzle sedimentation) and incorporates a detailed representation of radiative processes (Morcrette, 1991). Since recently, the model disposes of a positive definite third order advection scheme based on a Piecewise Parabolic Method (Colella and Woodward, 1986) which is used to advect the moist conservative variables, i.e. $\theta_l$ and $q_t$.

### 2.2 Boundary conditions

The three pairs of simulations consist of one with constant sea surface temperatures (SST) and large scale divergence, another with time varying SSTs and fixed divergence, and a third with both the SSTs and the divergence varying in time. The latter perhaps most realistically represents the evolution of boundary layer air masses as they circumnavigate the summertime subtropical high-pressure zones. The base values of the SST and divergence are taken as 288 K and $6\times10^{-6}\,\mathrm{s}^{-1}$, respectively. When allowed to vary SST is increased at a rate of $1.5\,\mathrm{K\,day}^{-1}$ and divergence is decreased by $1\times10^{-6}\,\mathrm{s}^{-1}\,\mathrm{day}^{-1}$, both changes being consistent with previous climatologies (Neiburger, 1960; Klein and Hartmann, 1993; Klein and Norris, 1995; Pincus et al., 1997).

#### 2.2.1 Initial conditions and large scale subsidence

The initialization of the simulations follows the EUROCS case (Duynkerke et al., 2004), although the initial profiles of $\theta_l$ and $q_t$ and the initial SST value are slightly modified so that the case with fixed boundary conditions behaves (in the pristine realization) quasi-periodically with a diurnal mean LWP of approximately 60–70 $\mathrm{g\,m}^{-2}$. This value is typical of marine stratocumulus over North-East Pacific during summertime (Wood et al., 2002).

Throughout the entire set of simulations, the only specified large scale forcing is the large-scale subsidence which is specified in terms of a fixed large-scale divergence (D), implying that $w_s=-Dz$ (where z is the height above the surface). Above the inversion, $w_s$ is set constant and equal to $-Dz_i$, $z_i$ being the maximum inversion height over the



ACPD
9, 5465–5503, 2009

domain. The influence of the subsidence on the temperature and the water content is accounted for via the source terms $w_s \frac{\partial \theta_l}{\partial z}$ and $w_s \frac{\partial q_t}{\partial z}$ in the equations for $\theta_l$ and $q_t$.

#### 2.2.2 Free tropospheric conditions

Maintaining the free tropospheric conditions nearly constant for the entire set of simulations allows to better emphasize the impact of varying subsidence rate and SST on the evolution of the boundary layer (Krueger et al., 1995; Wyant et al., 1997). For the simulations presented here, there is a slight imbalance between the subsidence warming and the net (diurnally averaged) radiative cooling within the free troposphere, but this causes only a slight drift in $\theta_l$ over time (of maximum 2–3 K after 72 h, as indicated by Fig. 2a). In order to maintain a steady-state for the free tropospheric water vapor during the entire period of simulation, we followed Krueger et al. (1995) approach. Thus, we choose an initial profile for $q_t$ which does not vary with height above the inversion (Table 1). This ensures the constancy of the free tropospheric $q_t$ over time, by maintaining the only sink term for moisture in this region, i.e. that is the subsidence drying source term ($w_s \frac{\partial q_t}{\partial z}$), equal to zero. Moreover, a sponge layer was imposed above 2000 m, and the thermodynamic profiles were relaxed toward the initial conditions at the upper boundary of the domain. The model setup and the initial conditions for the three pairs of simulations are summarized in Table 1, while the resulting STBL bulk variables and fluxes values are reported in Table 2.

### 2.3 Description of the simulations

#### 2.3.1 Non-precipitating clouds

The case with time invariant forcings features a pronounced diurnal cycle, though with a progressive damping of the cycle amplitude and a decline of the daily mean LWP (Fig. 1a). Figure 2 reveals that over the 72 h of simulation both $\theta_l$ and $q_t$ do not change noticeably, although the height of the boundary layer slightly decreases with time.



ACPD
9, 5465–5503, 2009



Title Page
Abstract | Introduction
Conclusions | References
Tables | Figures
◀◀ | ▶▶
◀ | ▶
Back | Close
Full Screen / Esc
Printer-friendly Version
Interactive Discussion

Letting the SST increase with time leads to stronger surface fluxes (Fig. 1b) and the boundary layer progressively warms and moistens (Fig. 2). Increased surface heat and moisture fluxes also strengthen the buoyancy flux, and the entrainment velocity increases slightly in response (Table 3). Overall the warming of the STBL dominates the moistening and the lifting condensation level rises faster than the cloud top, thus the LWP therefore diminishes gradually (Fig. 1a). This case behaves similarly to the case of Wyant et al. (1997) which was forced similarly.

In the case when the divergence is also allowed to gradually weaken with time, the growth of the boundary layer is (as expected) even more pronounced through the course of the simulation (Fig. 2). The thermodynamic state of the STBL largely follows the same evolution as in the case with only time-varying SSTs, but given that the STBL is deeper the cloud thickens relative to the previously described case (Fig. 1a). The most significant difference arising from the progressive weakening of the subsidence is the development of larger differentiation between the cloud and subcloud layer total-water specific humidity, which appears to be associated with the tendency of the more rapidly deepening layer to more strongly decouple (Fig. 2), and entrain somewhat more rapidly (e.g., Table 3). The reason for it to entrain more rapidly is unclear, but may be related to a thicker cloud layer.

Figure 3 provides information about the buoyancy fluxes for the three cases (grey points for the non-precipitating cases). The information is summarized in the decoupling parameter that is defined as the ratio of the negative to the positive areas of the buoyancy flux vertical profile in the boundary layer, i.e., the Buoyancy Integral Ratio, (Turton and Nicholls, 1987; Bretherton and Wyant, 1997; Stevens, 2000a). High values of this parameter indicate that turbulence forced by surface or radiative fluxes is increasingly dissipated in its effort to maintain a well-mixed layer. Both the case with fixed boundary conditions and the case with time-varying SSTs and divergence exhibit a significant decoupling during the day (from 10:00 to 16:00 LT). In contrast, the decoupling in the case where only the SSTs vary in time is less pronounced and almost disappears after 60 h of simulation. This feature corroborates previous work



ACPD
9, 5465–5503, 2009
Vertical structure and aerosol effects on stratocumulus
I. Sandu et al.

(Bougeault, 1985; Bretherton and Wyant, 1997) showing that deeper STBLs are often more decoupled, but it also reveals that decoupling is not a necessary condition for a decrease of the LWP.

#### 2.3.2 Precipitating clouds

At first glimpse, the precipitating cases behave like the non-precipitating ones (Table 3): the case with fixed forcings develops a slowly shallowing boundary layer, while the boundary layer top in the other simulations progressively increases albeit not as rapidly as in the cases with a polluted aerosol. The LWP evolves similarly among the three cases as before. Note, however, that because of its decreasing LWP, the precipitation in the SST case is inhibited during the third day of simulation (Fig. 4b).

Systematic, or robust differences between pairs of precipitating and non-precipitating representations of a particular scenario are evident in the daily mean LWP value and the amplitude of the LWP diurnal variation (Table 3). The mean LWP values are higher and the amplitude of the diurnal cycles are lower in the precipitating simulations, compared to the non-precipitating ones, on days 2 and 3, an exception being the last day of the case with only time-varying SSTs. The first day is disregarded because of the spin-up period that follows the sudden increase of CDNC at 00:00 LT. As mentioned above, day 3 for the case with time-varying SST shows a different response because precipitation is no longer active.

This contrasting features of the precipitating versus non-precipitating STBLs were discussed in Sandu et al. (2008). When drizzle is efficient the boundary layer does not entrain as much (Table 3), and tends to remain shallow and moist, if anything decoupling during the night due to the evaporation of precipitation below cloud base (Fig. 3). In the day a weak drizzle flux continues to contribute to less entrainment and evaporates near cloud base, counteracting the tendency of the layer to diurnally decouple. The precipitating STBLs are thus less decoupled during the daytime hours than the non-precipitating ones (Fig. 3). Thus, as long as the cloud precipitates, the diurnal cycle of the STBL is reduced, and its LWP is reinforced (Fig. 4a), compared to a non-precipitating STBL exposed to the same external forcings. These features are evident to some degree in each pair of simulations in Fig. 3, and thus this basic mechanism, does not appear sensitive to the details of the state of the STBL.

In summary, an aerosol second indirect effect has been simulated, where increased CCN enhances CDNC and inhibits drizzle precipitation in the STBL. In these simulations, droplet and drizzle sedimentation appears to be important at two levels : at cloud top where it attenuates the entrainment of free tropospheric air, and below cloud base where it modulates the degree of decoupling of the STBL and thus moderates the amplitude of the diurnal cycle. Because such effects would seem to be dependent on the vertical coupling of the STBL it is interesting to ask how well a model that does not well represent this coupling is able to capture the differences between pristine and polluted clouds. In other words, how important is it for large scale models to accurately represent the evolution of the STBL vertical structure if they are to be expected to capture the effects of the aerosol on cloud amount.

## 3 Vertical structure and cloud bulk properties

To begin we first investigate whether the difference in LWP between a pristine and a polluted cloud represented by LES can be captured while the departures from the mixed layer idealized state are neglected. We recall that in the simplest 0-D cloudy boundary layer model, i.e. the mixed layer model, the conservative variables, $\theta_l$ and $q_t$, are by definition constant with altitude through the depth of the boundary layer. To compare the LWP that would have been produced had the simulations remained well mixed with the results of the 3-D simulations, we construct what we call an equivalent mixed layer (EML). That is a vertically uniform (in $\theta_l$ and $q_t$) column, with the same depth as the mean 3-D STBL, the same mass of dry air and of water, hence same moist static energy. The EML is calculated for the entire set of simulations, at intervals of 10 min. Once $\theta_l$ and $q_t$ have been defined it is then possible to derive the EML cloud base and LWP, and to compare them with the mean 3-D LES ones.

Figure 5 compares the mean LWP of the LES simulations to the LWP of the EMLs, for the entire set of simulations, from 12:00 LT on the first day to the end of the simulations. Each point represents an hourly mean of the respective quantities. This figure suggests that the EML often provides a satisfactory diagnostic of the LWP. Some values, however, are significantly overestimated, especially for the periods when the polluted or the pristine simulated STBLs are decoupled (grey and black stars). The EML never underestimates the amount of liquid water as deviations from a well mixed state are always such that they tend to raise the condensation level, and therefore thin the cloud. In fact, the overestimation of the LWP in the EML is expected since in the STBL the moisture from the surface accumulates at the lowest levels, while dry air is entrained at cloud top. Turbulent mixing then partially neutralizes this moisture gradient. Since the same amount of total water is by definition uniformly distributed throughout the vertical in the EML, this layer is moister than its mean LES counterpart in the upper part of the STBL, and its LWP is overestimated. When the STBL is decoupled, turbulent mixing is less efficient, the moisture gradient in the LES simulation is less efficiently neutralized, and the discrepancy with the EML is more pronounced (Fig. 5).

The real question is however, whether or not the mixed layer assumption can capture the sensitivity of the liquid water path to the aerosol, as simulated by the LES. As a first step in answering this question the EML LWP difference between the PRIS and POL simulations, for the case with fixed forcings, is superimposed in Fig. 4a. This set of simulations presents the most marked differences between the precipitating and the non-precipitating clouds. The figure reveals that the ML assumption slightly underestimates the LWP difference during the day, more specifically from 10:00 to 16:00 LT, while it significantly overestimates it at nighttime and in the early morning. These time periods also correspond to contrasting values of the decoupling criterion, between the PRIS and POL simulations (Fig. 3). The discrepancy in the diagnosis of the LWP difference is less noticeable during daytime because, in both simulations, the LWP is significantly reduced compared to nighttime.

The overall impact is shown in Fig. 6, where the LWP difference between PRIS and

POL EML calculations is plotted against the one of the LES for the three pairs of simulations. It appears that when both STBLs are well-mixed (black dots), the EML reproduces the sign of the difference in LWP between the pristine and the polluted cloud. Meanwhile, this difference is noticeably overestimated during the nighttime periods when the pristine STBL is decoupled while the polluted one is well-mixed (green stars). During the periods when the polluted STBL only (orange stars) or both STBLs (red stars) are decoupled, which mostly correspond to daytime conditions, the difference in LWP between the two clouds is underestimated, and in some cases it is even reversed. The most serious drawbacks of the ML framework are exemplified here, where it appears that the sign of the LWP difference between a pristine and a polluted STBL is not always correctly diagnosed when the vertical structure is not accounted for.

## 4 Vertical structure and fluxes at the interfaces

A second question, is whether or not a model that fails to account for the structure of thermodynamic variables within the layer (i.e., a mixed-layer model (MLM)) might be expected to properly predict the evolution of the difference in LWP between a pristine and a polluted cloud, despite of the fact that it does not capture the differences in vertical structure between the two STBLs.

To answer this we first need to understand how sensitive the boundary fluxes, including the surface, entrainment and radiative fluxes, of the MLM are to the assumed vertical structure. Indeed, the divergence of these fluxes controls the evolution of the mixed-layer bulk state as follows:

$$\left(\frac{d\phi}{dt}\right)_{ML} = -\frac{\overline{w'\phi'}(z_i) - \overline{w'\phi'}(0)}{z_i - z(0)}, \qquad (1)$$

where $\phi=\{\theta_l, q_t\}$. The fluxes at the boundaries: $\overline{w'\phi'}(z_i)$ and $\overline{w'\phi'}(0)$, at the inversion



ACPD
9, 5465–5503, 2009

level $z_i$ and at the surface, respectively are given by:

$$\overline{w'\theta_l{}'}(z_i) = -w_e \Delta\theta_l + \frac{\Delta F_R}{\rho_l C_{pd}},$$
$$\overline{w'\theta_l{}'}(0) = H + L_v/C_{pd} F_p(0),$$
$$\overline{w'q_t{}'}(z_i) = -w_e \Delta q_t,$$
$$\overline{w'q_t{}'}(0) = LE + F_p(0), \tag{2}$$

where $w_e$ is the entrainment rate, $\Delta\theta_l$ and $\Delta q_t$ are the jumps in $\theta_l$ and $q_t$ at the inversion, H and LE are the sensible and latent heat fluxes at the surface, $F_p(0)$ is the precipitation flux at the surface (<0), $L_v$ is the enthalpy of vaporisation, $C_{pd}$ is the isobaric specific heat capacity of dry air and $\Delta F_R$ is the divergence of the upward net radiative flux across the mixed layer.

In what follows we will therefore explain how the fluxes at the boundaries of the EMLs are computed, and which are the sources of errors inherent to the ML assumption. Then, we will discuss the errors on the prediction of the LWP induced by using the EMLs fluxes instead of those of the mean 3-D STBL. Finally, we will get back to the central question of how these errors impact our ability to predict differences in the evolution of the LWP between pristine and polluted clouds.

### 4.1 Flux calculation in the EML

#### 4.1.1 Surface fluxes

The surface sensible and latent heat fluxes are proportional to the differences in $\theta_l$ and $q_t$ between the ocean surface and the atmosphere just above. They are derived using the same formulation as in the LES simulations, except for the $\theta_l$ and $q_t$ values at the bottom of the column that are those of the EML.

### 4.1.2 Radiative fluxes

The vertical profiles of the radiative fluxes within the EML are computed with an off-line version of the radiative transfer code of Meso-NH, assuming that the cloud optical properties are the same as in the LES simulations. For these computations two additional assumptions are made. First, we specify that above the well-mixed layer the properties of the atmosphere are identical to those of the mean LES column simulated at that time. Second, the CDNC is kept constant from the cloud base to the top and equal to the CDNC value simulated at that time, averaged over LES model grid cells where it is greater than $20\,\mathrm{cm}^{-3}$. The calculated profiles of the radiative fluxes are then used to derive the divergence of the upward net radiative flux across the boundary layer (solar plus infrared), taken as the difference between the value of the upward net flux above the EML and its value at the surface.

### 4.1.3 Entrainment rate

For the entrainment rate, several parameterizations (Turton and Nicholls, 1987; Konor and Arakawa, 2001; Lock, 1998; Moeng, 2000; Lilly, 2002; Lilly and Stevens, 2008) are tested, some of them including the liquid water sedimentation effect on cloud top entrainment (Bretherton et al., 2007). Those that do the best at reproducing the LES results are summarized in Table 4. They have all been formulated following the ML theory outlined in Stevens (2002). These parameterizations were initially developed for nocturnal conditions (no solar radiation). For application to the diurnal cycle, we therefore consider that the divergence of the radiative flux across the boundary layer top is equal to the divergence of the net upward total (solar plus thermal infrared) radiative flux (i.e. the difference between the value of the upward net flux above the inversion and its minimum value within the boundary layer).

For evaluation, the entrainment parameterizations are initialized with the horizontally averaged LES values of surface fluxes, radiative divergence at cloud top, which includes both solar and infrared fluxes, and jumps in $\theta_l$ and $q_t$ at cloud top. Over the entire set of PRIS and POL simulations they show relatively high correlation coefficients and small biases (except for the Konor and Arakawa (2001); Bretherton et al. (2007) parameterizations, which we do not explore further) (Table 4). The Turton and Nicholls (1987) parameterization has the smallest bias, a high correlation, and the smallest relative errors for both pristine and polluted cases, although it fails to reproduce correctly the difference in entrainment rates between pristine and polluted clouds (i.e. the averaged relative difference in entrainment rates between pristine and polluted clouds is of −16% in the LES and of +2% with the Turton and Nicholls (1987) parameterization). Keeping this caveat in mind (as it will become important latter) our further evaluation of the mixed layer theory is developed based on the Turton and Nicholls (1987) parameterization.

Our results thus suggest that the effects of the liquid water flux on the entrainment rate can be captured by a parameterization that does not include the direct effects of sedimentation, in so far as they are reflected in the underlying energetics which is used to derive the parameterized entrainment rates. For example, our interpretation of the good behavior of the original Turton and Nicholls (1987) parameterization is that the effects of the liquid water fluxes are captured, both through changes to the liquid water profile and to the buoyancy flux, which are naturally reproduced by the LES and which are then used as input parameters for the entrainment scheme. We recall that, as we noted above, the parameterized entrainment rates were computed here by using as an input the different horizontally mean LES output fields.

The heat and moisture fluxes at the boundary layer top are derived following Eq. (2), where the values above the EML, for the specification of the $\theta_l$ and $q_t$ jumps through the inversion, are taken from the mean values of the LES.

## 4.2 Process wise impacts of the mixed layer assumptions

### 4.2.1 Surface fluxes

When the simulated STBL is decoupled, the subcloud layer is colder and moister than the cloud layer, so that the EML $\theta_l$ and $q_t$ values are therefore greater, and respectively smaller than the horizontally averaged LES $\theta_l$ and $q_t$ values at the surface. The surface sensible heat flux of the EML is therefore slightly weaker than the LES one, while the surface moisture flux is stronger.

### 4.2.2 Radiative fluxes

The discrepancies in the radiative fluxes between the EMLs and the LES simulations cumulate three sources of errors. First, it has been shown in the previous section that the LWP is generally overestimated by the EML, especially when the STBL is decoupled. The corresponding flux divergence is accordingly overestimated. Second, the liquid water content (LWC) vertical profile is adiabatic by definition in the EML, with its maximum value at cloud top, while the mean LES LWC profiles exhibit a slightly lower maximum due to entrainment of dry air through the inversion layer. When precipitation is active, droplet and drizzle sedimentation tend to further lower the level of the LWC maximum (Sandu et al., 2008). Third, the mean radiative flux divergence of the LES is different from the flux divergence calculated with the mean LES fields because radiative transfer is non linear and the LWP is heterogeneous horizontally (heterogeneous radiative bias (Barker and Davies, 1992)). The same bias thus occurs in the EML that is derived from the mean LES fields.

### 4.2.3 Entrainment rate

The diagnosis of the entrainment rate is the most sensitive step in boundary layer models because it involves the energy fluxes at both the lower and upper interfaces, as well as the radiative fluxes to predict the generation of turbulent kinetic energy and the entrainment velocity. Noticeable discrepancies in the jumps of the conservative variables $\theta_l$ and $q_t$ across the inversion, between the LES and the EML also contribute to errors on the entrainment rates, especially when the STBL is decoupled, and or heavily precipitating.

When the entrainment rate is computed using the surface fluxes, the radiative divergence at cloud top and the bulk properties of the EML instead of those of the mean LES column, noticeable errors thus appear. For the Turton and Nicholls (1987) parameterization, the correlation coefficient is reduced to 0.78 and the relative error raises to +20% for the pristine cases. The relative error for the polluted clouds however is not affected and the bias is slightly improved (+0.007).

### 4.3 Effects on the prediction of the difference in LWP between pristine and polluted clouds

To measure the impact of the vertical structure on the prediction of the LWP, we evaluate here the errors in the LWP tendency (expressed in $\mathrm{g\,m^{-2}\,s^{-1}}$) that are introduced by using the fluxes at the boundaries of the EMLs instead of those at the boundaries of the mean 3-D STBLs.

The errors on the heat and moisture fluxes at the boundaries, when using the ML assumption, result in errors on the heating ($\delta\left(\frac{d\theta_l}{dt}\right)$), and moistening ($\delta\left(\frac{dq_t}{dt}\right)$) rates (not shown), hence in errors on the LWP tendency. The fluxes to consider are the surface sensible heat flux (H), the surface latent heat flux (LE), the surface precipitation heat flux (H PP), the surface precipitation latent heat flux (LE PP), the inversion heat ($\overline{w'\theta_l'}(z_i)$) and moisture ($\overline{w'q_t'}(z_i)$) fluxes. To separate their respective contributions, the error on the LWP tendency is calculated for each flux separately, as the LWP change induced by either $\delta\left(\frac{d\theta_l}{dt}\right)\Big|_{q_t}$ or $\delta\left(\frac{dq_t}{dt}\right)\Big|_{\theta_l}$.

Figures 7a and 7b summarize all the sources of errors for the pristine and the polluted simulations of the case with fixed boundary conditions with the contributions of each flux and the total error. It appears that the total error is more important in the pristine case (Fig. 7a), due mainly to larger errors on the turbulent fluxes at the boundary layer top, i.e. larger errors on the entrainment rates (Sect. 4.2.3). Furthermore, the errors appear to be somewhat larger at night, when drizzle is effective in decoupling the boundary layer as represented by the LES. In the polluted case, the errors associated to each flux are smaller and they largely counterbalance one another, so that the total error on the LWP tendency is mostly smaller (Fig. 7b), albeit of opposite sign. This changing of sign may impact the sensitivity of the mixed layer model to the character of the aerosol.

Note, however, that there is no precipitation parameterization in the MLM. The errors shown in the figure for the precipitation flux thus correspond to the LES contribution alone. In an attempt to also include a diagnostic of the precipitation flux at the surface in the MLM, we use an empirical parameterization similar to the one proposed by Geoffroy et al. (2008) for the precipitation flux at cloud base, but based on an empirical fit to the values of the precipitation flux at the surface from our simulations. The total error on the LWP tendency is not improved and even increases. This is due to the overestimation of the LWP in the EML, that has been shown to be mostly noticeable when the STBL is decoupled. In the precipitating case, this LWP overestimation results in an overestimation of the precipitation flux at the surface.

These results show that the errors on the LWP tendency made in pristine and polluted cases do not have the same sign, nor the same magnitude, and therefore suggest that a noticeable error will be made on the prediction of the difference in LWP between two such clouds if the ML theory is used to compute the fluxes at the boundaries. Moreover, one observes that the ML assumption underestimates the LWP tendency when the cloud layer is precipitating. That bias might counterbalance the tendency of the ML framework to overestimate the LWP when the boundary layer is decoupled, as discussed in the previous section. To test such a hypothesis, we now let the MLM evolve freely, based on its own parameterizations.

## 5 Performance evaluation of the MLM

### 5.1 Methodology

For both the pristine and the polluted case, the MLM is initialized with the EML derived at 12:00 LT on the first day of simulation (for each of the three pairs of simulations). Its evolution is then computed, with a time step of 10 min, using Eqs. (1) and (2), with the Turton and Nicholls (1987) parameterization for the entrainment rate. At each time step, the fluxes at the boundaries (computed as indicated in Sect. 3.2) are thus used to derive the heating and the moistening rates of the mixed layer and the evolution of the conservative variables. In the meantime, the rate of growth of the mixed layer is computed as the difference between the entrainment rate and the subsidence rate (equal to that imposed in the LES at that time). The bulk properties are then used to diagnose the LWP.

For the pristine cases, two such integrations are performed. In the first one, the precipitation is not parameterized, while in the second, we use the same empirical parameterization of the precipitation flux at the surface as described above.

### 5.2 Results

Figure 8a shows the time evolution of the difference in LWP between the PRIS and the POL LES performed in the case with fixed boundary conditions (full line) and the difference in LWP obtained from the integrations of the MLM, with (dotted) and without (dashed) precipitation at the surface in the PRIS case.

The sign of the difference in LWP between a pristine and a polluted STBL predicted by the MLM is always the opposite of the one predicted with LES, and the bulk parameterization of the precipitation at the surface does not improve the results. Thus, contrary to the results of the LES, the MLM predicts that the polluted cloud always contains more water than the pristine one, and this tendency is the same for the three sets of simulations (Fig. 9). Indeed, the MLM almost always overestimates the LWP of the polluted cloud and underestimates the LWP of the pristine one (Fig. 8b). These differences are consistent with the differences we saw in the diagnostic evaluation of the mixed-layer model, wherein the biases in entrainment tended to moisten the polluted clouds and dry the pristine ones, in contradiction to the LES results.

## 6 Conclusions

Three sets of 72 h LES of marine stratocumulus have been performed to cover a broad range of external forcings, in term of sea surface temperature and subsidence from above. Each set comprises a pair of simulations, the first one with a low CCN concentration, hence a low CDNC, that mostly precipitate, and the second one with a higher CCN concentration, hence greater CDNC, in which precipitation is inhibited. To varying degrees these simulations show that the LWP of the non-precipitating boundary layer is lower than the LWP of a precipitating one exposed to the same external forcings, quite in contrast to the simple models often introduced to explore indirect effects of the aerosol (Quaas et al., 2004; Lohmann and Feichter, 2005).

Given these simulations we then ask the question: Would the simplest, consistent model of the marine boundary layer (i.e., the mixed layer model) be able to replicate this behavior of the LES? To answer this question each simulation has been analyzed and the bulk properties of the mixed layer equivalent to the mean 3-D STBL have been derived, at 10 min intervals. These equivalent profiles have then been used to diagnose the LWP one would expect to find in a mixed layer with the same mean state. Not, surprisingly, the EML overestimates the LWP compared to its LES counterpart, especially when the LES simulated boundary layer is decoupled. As the decouplings appear at different times of the day in a precipitating and a non-precipitating STBL and their intensities are also different, the difference in LWP between the two clouds is not correctly diagnosed with the ML assumption. That said the biases are systematic in that they impact both the pristine and polluted simulations similarly, albeit not commensurately.

The parameterizations of the energy fluxes at the interfaces, that have been devel-



ACPD
9, 5465–5503, 2009

oped for boundary layer schemes, have then been evaluated. We also evaluated the parameterization of the entrainment rate at cloud top, as this has long been an issue of concern. We find that biases in the representation of entrainment by the mixed layer framework are most strongly related to the presence of precipitation, either via the modification of the LWC vertical profile by droplets and drizzle drops sedimentation, or via the release of latent heat due to drizzle evaporation below cloud base. As a consequence, the warming and the drying of the STBL associated with cloud top entrainment is overestimated by the mixed-layer model when precipitation is active, hence the LWP tendency is underestimated.

To investigate which one of these two contrasting tendencies dominates, i.e. the LWP overestimation for a specified bulk state of the boundary layer, and the underestimation of the LWP evolution, the MLM has been allowed to evolve freely, based on its own parameterizations. In this case, the LWP of the precipitating boundary layer is systematically underestimated (indicative of too much entrainment), while the one of the non-precipitating STBL is overestimated, so that the sign of the difference in LWP between the two clouds is the opposite of what the LES indicate.

This exercise therefore suggests that, to reduce the uncertainty of aerosol indirect effects in climate change predictions, it is necessary to accurately represent the vertical structure within the boundary layer. The deviations from the mixed layer state, their modulation by precipitation, as well as their impacts on the energy fluxes at the boundary layer interfaces should therefore be accounted for in future in the schemes of cloudy boundary layers included in the large scale models.

*Acknowledgements.* Irina Sandu, Odile Thouron, and Jean-Louis Brenguier acknowledge the support of Météo-France and CNRS. This work has been partly funded by EUCAARI (European Integrated project on Aerosol Cloud Climate and Air Quality interactions) No. 036833-2.

This Open Access Publication is financed by CNRS-INSU and the Max Planck Society.

ACPD

9, 5465–5503, 2009

Vertical structure and aerosol effects on stratocumulus

I. Sandu et al.

Title Page | Abstract | Introduction | Conclusions | References | Tables | Figures | Back | Close | Full Screen / Esc | Printer-friendly Version | Interactive Discussion

## References

Ackerman, A. S., Kirkpatrick, M. P., Stevens, D. E., and Toon, O. B.: The impact of humidity above stratiform clouds on indirect aerosol climate forcing, Nature, 432, 1014–1017, 2004. 5468

Albrecht, B.: Effects of Precipitation on the Thermodynamic Structure of the Trade Wind Boundary Layer, J. Geophys. Res., 98(D4), 7327–7337, 1993. 5467

Barker, H. and Davies, J. A.: Solar radiative fluxes for stochastic, scale-invariant broken cloud fields, J. Atmos. Sci., 49, 1115–1126, 1992. 5481

Bougeault, P.: The diurnal cycle of marine stratocumulus: A higher order model study, J. Atmos. Sci., 42, 2826–2843, 1985. 5474

Bretherton, C. S. and Wyant, M. C.: Moisture transport, lower-troposphere stability, and decoupling of cloud-topped boundary, J. Atmos. Sci., 54, 148–167, 1997. 5467, 5473, 5474

Bretherton, C. S., Blossey, P. N., and Uchida, J.: Cloud droplet sedimentation, entrainment efficiency, and subtropical stratocumulus albedo, Geophys. Res. Lett., 34, L03813, doi:10.1029/2006GL027648, 2007. 5468, 5479, 5480

Caldwell, P., Bretherton, C. S., and Wood, R.: Mixed-Layer Budget Analysis of the Diurnal Cycle of Entrainment in Southeast Pacific Stratocumulus, J. Atmos. Sci., 62, 3775–3791, 2005. 5467

Cohard, J. M., Pinty, J. P., and Shure, K.: On the parameterization of activation spectra from cloud condensation nuclei microphysical properties, J. Geophys. Res., 105, 11753–11766, 2000a. 5470

Colella, P. and Woodward, P. R.: The Piecewise Parabolic Method (PPM) for Gas-Dynamical Simulations, J. Comput. Phys., 54, 174–201, 1986. 5471

Duynkerke, P. G., de Roode, S. R., van Zanten, M. C., Calvo, J., Cuxart, J., Cheinet, S., Chlond, A., Grenier, H., Jonker, P. J., Kohler, M., Lenderink, G., Lewellen, D., Lappen, C.-L., Lock, A. P., Moeng, C.-H., Muller, F., Olmeda, D., Piriou, J.-M., Sanchez, E., and Sednev, I.: Observations and numerical simulations of the diurnal cycle of the EUROCS stratocumulus case, Q. J. Roy. Meteor. Soc., 604, 3269–3296, 2004. 5471

Feingold, G., Stevens, B., Cotton, W. R., and Frisch, A. S.: On the relationship between drop in-cloud residence time and drizzle production in stratocumulus clouds, J. Atmos. Sci., 53, 1108–1122, 1996. 5468

Geoffroy, O.: Modélisation LES des précipitations dans les nuages de couche limite et paramétrisation pour les modèles de circulation générale, Thèse de Doctorat, 2007. 5470

Geoffroy, O., Brenguier, J.-L., and Sandu, I.: Relationship between drizzle rate, liquid water path and droplet concentration at the scale of a stratocumulus cloud system, Atmos. Chem. Phys., 8, 4641–4654, 2008, http://www.atmos-chem-phys.net/8/4641/2008/. 5483

Khairoutdinov, M. and Kogan, Y.: A New Cloud Physics Parameterization in a Large-Eddy Simulation Model of Marine Stratocumulus, Mon. Weather Rev., 128, 229–243, 2000. 5470

Klein, S. A. and Hartmann, D. L.: The Seasonal Cycle of Low Stratiform Clouds, J. Climate, 6, 1587–1606, 1993. 5471

Klein, S. A. and Norris, J. R.: On the Relationships among Low-Cloud Structure, Sea Surface Temperature, and Atmospheric Circulation in the Summertime Northeast Pacific, J. Climate, 8, 1140–1155, 1995. 5470, 5471

Konor, C. and Arakawa, A.: Incorporation of moist processes and a PBL parameterization into the generalized vertical coordinate model, Technical report 102, UCLA, Department of Atmospheric Sciences, Box 951565, Los Angeles CA 90095-1565, 66 pp., 2001. 5479, 5480

Krueger, S. K., McLean, G. T., and Fu, Q.: Numerical Simulation of the Stratus-to-Cumulus Transition in the Subtropical Marine Boundary Layer. Part I: Boundary-Layer Structure, J. Atmos. Sci., 52, 2839–2850, 1995. 5472

Lafore, J. P., Stein, J., Asencio, N., Bougeault, P., Ducrocq, V., Duron, J., Fischer, C., Héreil, P., Mascart, P., Masson, V., Pinty, J. P., Redelsperger, J. L., Richard, E., and Vilà-Guerau de Arellano, J.: The Meso-NH Atmospheric Simulation System. Part I: adiabatic formulation and control simulations, Ann. Geophys., 16, 90–109, 1998, http://www.ann-geophys.net/16/90/1998/. 5470

Lilly, D. K.: Models of cloud topped mixed layers under a strong inversion, Q. J. Roy. Meteor.



ACPD

9, 5465–5503, 2009

Vertical structure and aerosol effects on stratocumulus

I. Sandu et al.

Soc., 94, 292–309, 1968. 5467, 5468
Lilly, D. K.: Entrainment into mixed layers. Part II: A new closure, J. Atmos. Sci., 59, 3353–3361, 2002. 5467, 5479, 5494
Lilly, D. K.: Validation of a mixed-layer closure. Part II: Observational tests, Q. J. Roy. Meteor. Soc., 134, 57–67, 2008. 5467
Lilly, D. K. and Stevens, B.: Validation of a mixed-layer closure. Part I: Theoretical tests, Q. J. Roy. Meteor. Soc., 134, 47–55, 2008. 5467, 5479, 5494
Lock, A.: The parameterization of entrainment in cloudy boundary layers, Q. J. Roy. Meteor. Soc., 124, 2729–2753, 1998. 5479, 5494
Lohmann, U. and Feichter, J.: Global indirect aerosol effects: a review, Atmos. Chem. Phys., 5, 715–737, 2005, http://www.atmos-chem-phys.net/5/715/2005/. 5485
Lu, M. L. and Seinfeld, J. H.: Study of the aerosol indirect effect by Large-Eddy Simulation of marine stratocumulus, J. Atmos. Sci., 62, 3909–3932, 2005. 5468
Moeng, C.: Entrainment rate, cloud fraction, and Liquid Water Path of PBL stratocumulus clouds, J. Atmos. Sci., 57, 3627–3643, 2000. 5479, 5494
Morcrette, J.: Radiation and cloud radiative properties in the ECMWF operational weather forecast model, J. Geophys. Res., 96, 9121–9132, 1991. 5471
Neiburger, M.: The relation of air mass structure to the field of motion over the eastern North Pacific Ocean in summer, Tellus, 12, 31–40, 1960. 5471
Nicholls, S.: The dynamics of stratocumulus, Q. J. Roy. Meteor. Soc., 110, 821–845, 1984. 5467
Pincus, R., Baker, M., and Bretherton, C.: What controls stratocumulus radiation properties? Lagrangian observations of cloud evolution, J. Atmos. Sci., 54, 2215–2236, 1997. 5470, 5471
Quaas, J., Boucher, O., and Bréon, F.-M.: Aerosol indirect effects in POLDER sattelite data and the Laboratoire de Météorologie Dynamique-Zoom (LMDZ) general circulation model, J. Geophys. Res., 109, D08205, doi:10.1029/2003JD004 317, 2004. 5485
Sandu, I., Brenguier, J. L., Geoffroy, O., Thouron, O., and Masson, V.: Aerosol impacts on the diurnal cycle of marine stratocumulus, J. Atmos. Sci., 65, 2705–2718, 2008. 5467, 5470, 5474, 5481
Savic-Jovcic, V. and Stevens, B.: The structure and mesoscale organization of precipitating stratocumulus, J. Atmos. Sci., 65, 1587–1605, 2008. 5468



ACPD
9, 5465–5503, 2009

Vertical structure and aerosol effects on stratocumulus

I. Sandu et al.

Schubert, W., Wakefield, J. S., Steiner, E. J., and Cox, S. K.: Marine Stratocumulus Convection. part II: Horizontally Inhomogeneous Solutions, J. Atmos. Sci., 36, 1309–1324, 1979. 5470

Stevens, B.: Cloud-transitions and decoupling in shear-free stratocumulus topped boundary layers, Geophys. Res. Lett., 27, 2557–2560, 2000a. 5467, 5473

Stevens, B.: Entrainment in Stratocumulus Topped Mixed Layers, Q. J. Roy. Meteor. Soc., 128, 2663–2690, 2002. 5467, 5479

Stevens, B.: Atmospheric Moist Convection, Annu. Earth Planet. Sci, 32, 605–643, 2005. 5467

Stevens, B., Cotton, W. C., Feingold, G., and Moeng, C.-H.: Large-eddy Simulations strongly precipitating, shallow, stratocumulus-topped boundary layers, J. Atmos. Sci., 55, 3616–3638, 1998. 5468

Turton, J. and Nicholls, S.: A study of the diurnal variation of stratocumulus using a multiple mixed-layer model, Q. J. Roy. Meteor. Soc., 113, 969–1011, 1987. 5467, 5473, 5479, 5480, 5482, 5484, 5494

Wood, R.: Cancellation of aerosol indirect effects in marine stratocumulus through cloud thinning, J. Atmos. Sci., 64, 2657–2669, 2007. 5467

Wood, R., Bretherton, C. S., and Hartmann, D. L.: Diurnal cycle of liquid water path over subtropical and tropcal oceans, Geophysical Res. Let., 29, 2092, doi:10.1029/2002GL015371, 2002. 5471

Wyant, M., Bretherton, C., Rand, H., and Stevens, D.: Numerical simulations and a conceptual model of the subtropical marine stratocumulus to trade cumulus, J. Atmos. Sci., 54, 168–192, 1997. 5472, 5473

Zhang, Y., Stevens, B., and Ghil, M.: On the diurnal cycle and susceptibility to aerosol concentration in a stratocumulus-topped mixed layer, Q. J. Roy. Meteor. Soc., 131, 1567–1583, 2005. 5467



ACPD

9, 5465–5503, 2009

Vertical structure and aerosol effects on stratocumulus

I. Sandu et al.

**Table 1.** Characteristics of the simulations.

| Type | Parameter | Value |
|---|---|---|
| Initial conditions | Latitude, longitude | 33°15′ N, 119°30′ W |
| | Local time | 21:00 LT for pristine, 00:00 LT for polluted simulations |
| | Surface reference pressure | 1012.5 mb |
| | Horizontal wind | geostrophic wind |
| | Geostrophic wind velocity, direction | $6\,m\,s^{-1}$, 305° |
| | Initial SST | 288 K |
| | Initial large scale divergence | $6\times10^{-6}\,s^{-1}$ |
| | Boundary layer $\theta_l$ | 285.5 K |
| | Boundary layer $q_t$ | $9.6\,g\,kg^{-1}$ |
| | Inversion level | 600 m |
| | Cloud top $\theta_l$ jump | 12 K |
| | Cloud top $q_t$ jump | $-3\,g\,kg^{-1}$ |
| | Free troposphere $\theta_l$ rate | $+7.5\,K\,km^{-1}$ |
| | Free troposphere $q_t$ rate | 0 |
| Numerics | Height | 3 km |
| | Width | 2.5×2.5 km |
| | Horizontal resolution | 50 m |
| | Vertical resolution | 10 m up to 900 m, slightly decreased above |
| | Number of vertical levels | 116 |
| | Boundary conditions | periodic |
| | Absorbing layer | above 2 km |
| | Duration | 75 h for pristine, 72 h for polluted simulations |
| | Time step | 1 s |



ACPD

9, 5465–5503, 2009

Vertical structure and aerosol effects on stratocumulus

I. Sandu et al.

**Table 2.** Range of variation of the key variables in the simulations: mean $\theta_l$ and $q_t$ over the STBL, maximum LWC, $\theta_l$, $q_t$ and buoyancy jumps at cloud top, sensible and latent heat fluxes at the surface, upward net radiative flux jump at cloud top, cloud fraction (a column is considered as cloudy if the LWP is bigger than $2\,\mathrm{g\,m^{-2}}$), inversion level, SST, and large scale divergence.

| Parameter | Range |
|---|---|
| $\overline{\theta_l}$ (K) | [286, 291.5] |
| $\overline{q_t}$ ($\mathrm{g\,kg^{-1}}$) | [8.7, 10.5] |
| $q_{l,\max}$ ($\mathrm{g\,kg^{-1}}$) | [0.14, 0.53] |
| $\Delta\theta_l$ (K) | [8.5, 11] |
| $\Delta q_t$ ($\mathrm{g\,kg^{-1}}$) | [−4, −2] |
| $\Delta b$ ($\mathrm{m^2\,s^{-3}}$) | [0.24, 0.32] |
| $\overline{w'\theta_l'}(0)$ ($\mathrm{W\,m^{-2}}$) | [−3, 8.5] |
| $\overline{w'q_t'}(0)$ ($\mathrm{W\,m^{-2}}$) | [10.7, 54.3] |
| $\Delta F$ ($\mathrm{W\,m^{-2}}$) | [26, 66.4] |
| cloud fraction | [0.85, 1] |
| inversion level (m) | [600,1000] |
| SST (K) | [288,292.5] |
| LS divergence ($\mathrm{s^{-1}}$) | [$3\times10^{-6}$, $6\times10^{-6}$] |

**Table 3.** Diurnal mean LWP ($g\,m^{-2}$), amplitude of the LWP diurnal cycle (A) ($g\,m^{-2}$) and diurnal mean entrainment rate $w_e$ ($cm\,s^{-1}$) for each day of simulation in the three scenarios, for polluted and pristine clouds.

| Parameter | Sim. | Fixed boundary conditions | | | time-varying SST | | | time-varying SST and divergence | | |
|---|---|---|---|---|---|---|---|---|---|---|
| | | Day 1 | Day 2 | Day 3 | Day 1 | Day 2 | Day 3 | Day 1 | Day 2 | Day 3 |
| $\overline{LWP}$ | POL | 65.7 | 53.3 | 51.7 | 64.4 | 39.7 | 26.4 | 67 | 55.1 | 53.9 |
| | PRIS | 65.2 | 66.7 | 64.3 | 61.4 | 45.2 | 26.1 | 64.2 | 59.1 | 61.8 |
| A | POL | 87 | 52.4 | 46.9 | 80.6 | 38.5 | 28.2 | 78.5 | 52.4 | 79.7 |
| | PRIS | 44.3 | 43.4 | 42.5 | 49.6 | 44.3 | 31.8 | 40.6 | 43.7 | 46.1 |
| $w_e$ | POL | 0.32 | 0.29 | 0.26 | 0.37 | 0.38 | 0.38 | 0.38 | 0.42 | 0.47 |
| | PRIS | 0.24 | 0.23 | 0.21 | 0.28 | 0.34 | 0.34 | 0.3 | 0.37 | 0.44 |



ACPD
9, 5465–5503, 2009

Vertical structure and aerosol effects on stratocumulus

I. Sandu et al.

**Table 4.** Overall bias and correlation coefficients over the entire set of simulations, and relative error for the pristine and polluted cases respectively.

| Parameterization | Bias ($cm\,s^{-1}$) | Correlation | Rel. error (%) POL | Rel. error (%) PRIS |
|---|---|---|---|---|
| Turton and Nicholls (1987) | −0.013 | 0.827 | −13 | 8 |
| Lock (1998) | −0.099 | 0.737 | −35 | −22 |
| Moeng (2000) | 0.062 | 0.765 | 12 | 33 |
| Lilly (2002) | −0.089 | 0.897 | −32 | −20 |
| Lilly and Stevens (2008) | −0.1 | 0.882 | −24 | −32 |



ACPD
9, 5465–5503, 2009

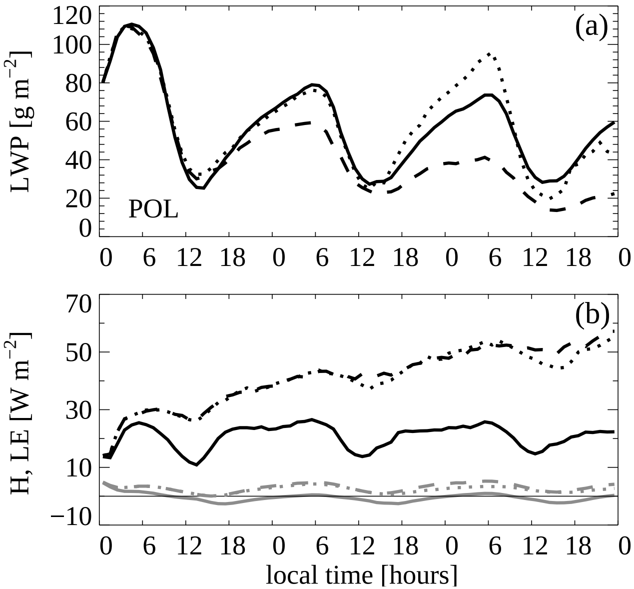


**Fig. 1.** Time evolution of the horizontal mean: **(a)** LWP (g m$^{-2}$) and **(b)** sensible (grey lines) and latent heat (black lines) fluxes at the surface (W m$^{-2}$) for the polluted STBLs simulated in the cases: with fixed boundary conditions (full), with time-varying SSTs (dashed) and with time-varying SSTs and divergence (dotted).



ACPD

9, 5465–5503, 2009

Vertical structure and aerosol effects on stratocumulus

I. Sandu et al.

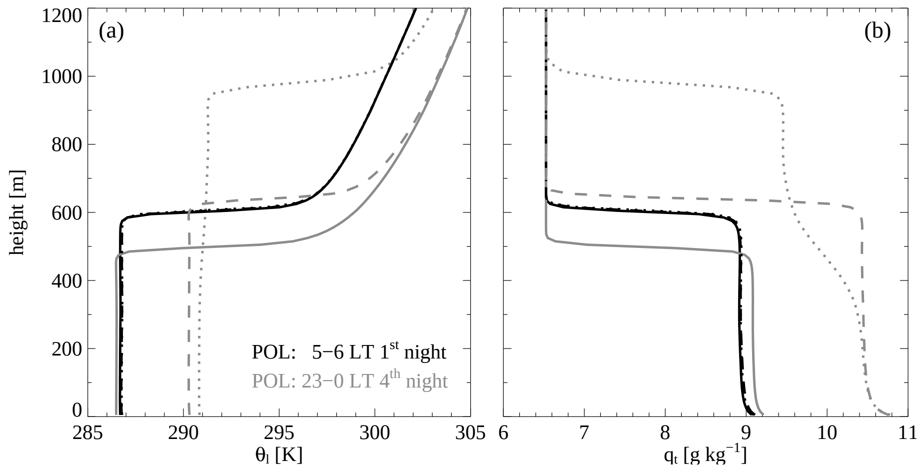


**Fig. 2.** Vertical profiles of the horizontal mean **(a)** liquid water potential temperature (K) and **(b)** total water mixing ratio (g kg$^{-1}$), averaged from 05:00 to 06:00 LT during the 1st night (black) and from 23:00 to 00:00 LT during the last night of simulation (grey). The full, dashed and dotted lines correspond to the polluted STBL simulated in cases with fixed boundary conditions, with time-varying SSTs and with time-varying SSTs and divergence, respectively.

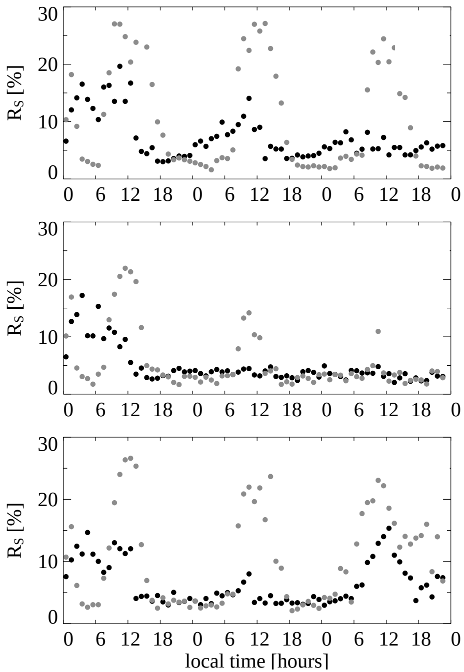


**Fig. 3.** Time evolution of the hourly averaged decoupling criterion $R_S$ (%) for the pristine (black) and polluted STBLs (grey). The upper, middle and lower panels correspond to the cases with fixed boundary conditions, with time-varying SSTs and with time-varying SSTs and divergence, respectively.



ACPD
9, 5465–5503, 2009



Title Page
Abstract | Introduction
Conclusions | References
Tables | Figures
◀| |▶
◀ ▶
Back | Close
Full Screen / Esc
Printer-friendly Version
Interactive Discussion

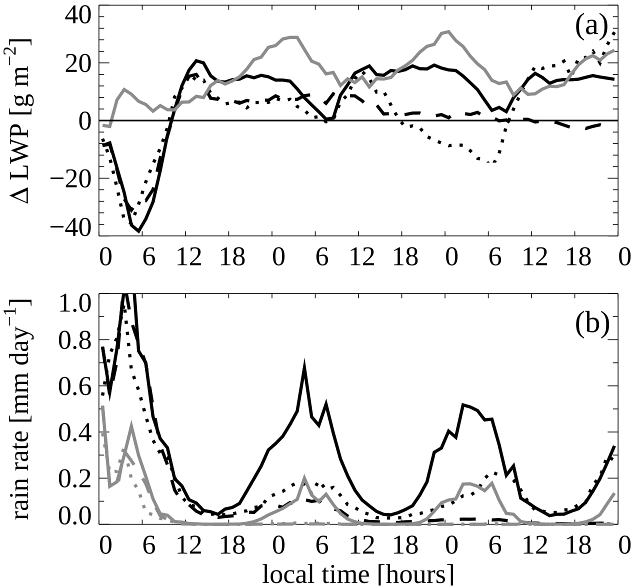


**Fig. 4.** Time evolution of **(a)** the difference in horizontal mean LWP ($g\,m^{-2}$) between the pristine and the polluted clouds and **(b)** the precipitation rates ($mm\,day^{-1}$) at sea level (grey) and at cloud base (black) for the pristine clouds simulated in the cases with fixed boundary conditions (full), with time-varying SSTs (dashed) and with time-varying SSTs and divergence (dotted), respectively. The full grey line in panel (a) shows the difference between the LWPs of the well-mixed layers equivalent to the pristine and polluted STBLs simulated in the case with fixed boundary conditions.

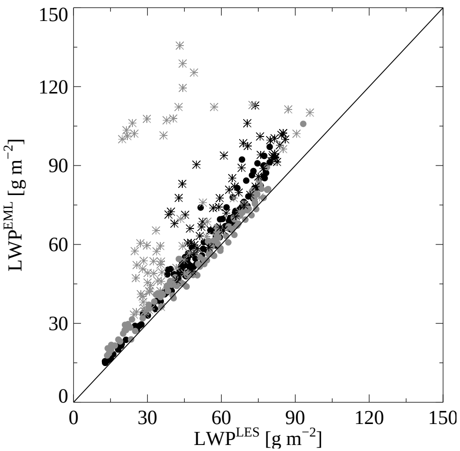


**Fig. 5.** EML LWP against the LES LWP ($g\,m^{-2}$). The black and grey symbols correspond to pristine and polluted cases, respectively. The dots and stars represent situations when the STBL is well-mixed and decoupled, respectively. A STBL is considered to be decoupled if $R_S$>5%.



ACPD
9, 5465–5503, 2009

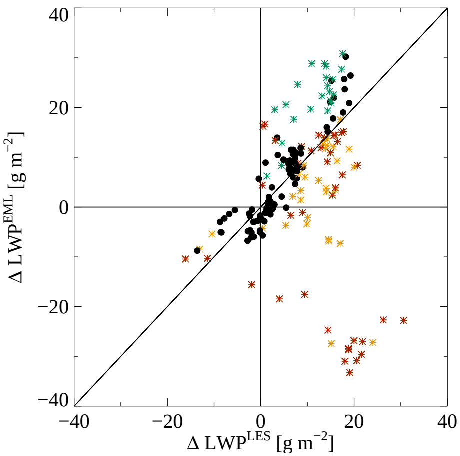


**Fig. 6.** Difference between the EML pristine and polluted LWPs against the difference between the LES ones ($g\,m^{-2}$). The black dots correspond to situations when both STBLs are well-mixed, while the stars correspond to cases when: only the pristine STBL is decoupled (green), only the polluted STBL is decoupled (orange), both STBLs are decoupled (red).

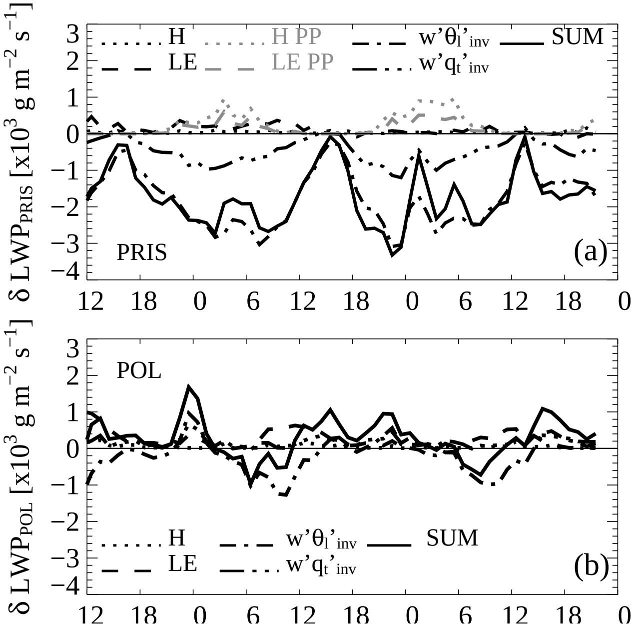


**Fig. 7.** Errors on the prediction of the LWP ($g\,m^{-2}\,s^{-1}$) tendency when using the ML assumption to compute the various fluxes at the boundaries, as listed in the legend, of **(a)** a pristine and **(b)** a polluted STBL, and the total error (full line) (for the case with fixed boundary conditions).

ACPD

9, 5465–5503, 2009

Vertical structure and aerosol effects on stratocumulus

I. Sandu et al.





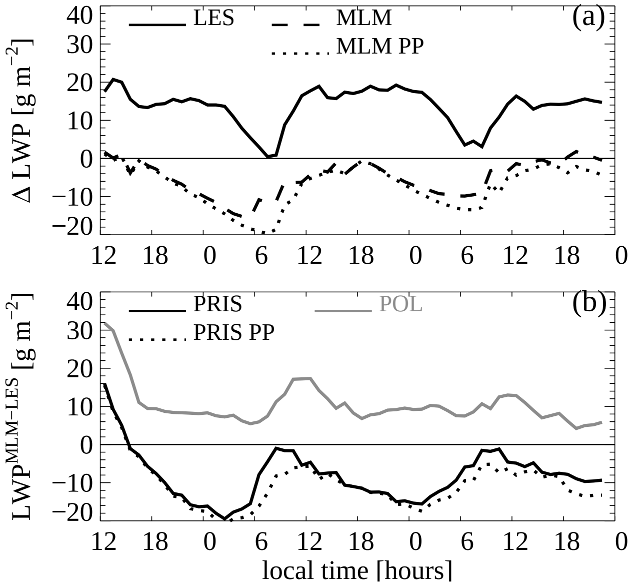


**Fig. 8.** **(a)** Time evolution of the difference between the LWPs of the pristine and the polluted STBLs, for the LES simulations in the case with fixed boundary conditions (full line) and for the corresponding integrations of the MLM, with (dotted) and without (dashed) parameterization of precipitation at the surface. **(b)** Time evolution of the difference in LWP between the MLM and the LES simulations for the polluted (grey) and for pristine STBLs (black) in the case with fixed boundary conditions. The dotted and full black lines correspond to integrations of the MLM with and without parameterization of precipitation at the surface, respectively.

ACPD

9, 5465–5503, 2009

Vertical structure and aerosol effects on stratocumulus

I. Sandu et al.



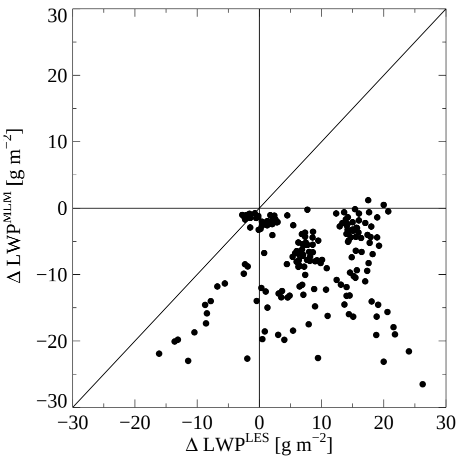


**Fig. 9.** Difference between the LWPs of the pristine and the polluted STBLs (hourly means, in $g\,m^{-2}$) predicted by the MLM against the same difference derived from the LES simulations for the three pairs of simulations.